SUBMITTED TO
NUOVO CIMENTO

CERN/TC/PHYSICS 65-6
18.2.1965

THE REACTION $KN\pi\pi$ AT 3 GEV/C AND THE PRODUCTION MECHANISM OF $K^{*}N^{*}$

M. Ferro-Luzzi, R. George, Y. Goldschmidt-Clermont, V.P. Henri, B. Jongejans, D.W.G. Leith, G.R. Lynch, F. Muller and J.-M. Perreau,

CERN, Geneva - Switzerland.

Abstract

In a study of the four particle states $K^{+}p \longrightarrow KN\pi\pi$ at 3 GeV/c, it is found that the quasi two-body process $K^{+}p \longrightarrow K^{*}N^{*}$ occurs in large proportion. The cross-sections for the various charge and decay modes of $K^{*}N^{*}$ are in good agreement with the predictions based on isotopic spin invariance. The sharply peaked c.m. production angular distribution suggests peripheralism. Within the framework of a simple one-meson exchange model the decay angular distributions of K^{*} and N^{*} are consistent with the assumption that the reaction proceeds predominantly through the exchange of a single pion. Such a model is unable to explain the non-zero value of the "interference" parameter Re $\rho_{1,0}$ (-0.13 ± 0.02). In addition, the model requires the inclusion of a drastic ad-hoc form factor, similar to the one used at 1.96 GeV/c, in order to fit the observed production angular distribution. A modified one-meson exchange model, taking into account the absorption due to competing processes and developed by Gottfried, Jackson, Keyser and Svensson, does not explain the absolute value of the cross-section, but predicts, with a minimum of assumptions, a production angular distribution and decay correlations in reasonable accord with experiment.

PS/4801/mhg

CERN/TC/PHYSICS 65-6
18.2.1965

THE REACTION $KN\pi\pi$ AT 3 GEV/C AND THE PRODUCTION MECHANISM OF $K^{*}N^{*}$

M. Ferro-Luzzi, R. George, Y. Goldschmidt-Clermont, V.P. Henri, B. Jongejans, D.W.G. Leith, G.R. Lynch, F. Muller and J.-M. Perreau,

CERN, Geneva - Switzerland

We report on the results of a study of the four-body final states $K^{+}p \rightarrow KN\pi\pi$ at 3 GeV/c, and in particular on the production mechanism of K^{*} and N^{*} in the $K^{+}p \rightarrow K^{*}N^{*}$ channel. Preliminary results on part of this study have been reported elsewhere[1].

1. Experimental Procedure

The Saclay 81 cm hydrogen bubble chamber was exposed at the CERN proton synchrotron to a separated K^{+} beam[2] with a momentum at the centre of the chamber of 2.97 GeV/c (total energy in the centre of mass $E_{tot} = 2.60$ GeV) and a dispersion of $\pm$ 0.015 GeV/c. The pion contamination of the beam was on the average not more than 5%. Approximately 10^{5} pictures were taken containing about 10^{6} beam tracks. They were scanned and re-scanned for, among other things, all interactions containing four charged prongs and all two-prong events associated with a V^{0}. In the case of the latter, a fiducial volume was chosen to eliminate events with large escape probability for the V^{0}. For the four-prong events, a smaller fiducial volume was chosen to reduce the number of events with poor resolution; furthermore, for the study of this topology we only used the films for which the pion contamination was found to be especially small.

The events were measured on the CERN IEP measuring projectors and processed through the CERN computer programs : THRESH (geometry), GRIND (kinematics) and BAKE (calculation of relevant dynamical quantities). For each event a verification was then made on the scanning table to see if the ionization of the tracks was consistent with the results of the fit. Events for which GRIND could not find an interpretation were processed with MILLSTONE, a program which allows

the user to guide GRIND in the performance of the kinematical analysis of individual events. As a result of this procedure, practically all the events were given an unambiguous interpretation.

Of the many possible final states, some have already been reported[3), 4)]. Here we shall discuss the following reactions :

$$K^+p \rightarrow K^+ p \pi^+ \pi^- \qquad \text{(1009 events);} \qquad (1)$$

$$K^+p \rightarrow K^o p \pi^+ \pi^o, \quad K^o \rightarrow \pi^+ \pi^- \qquad \text{(739 events);} \qquad (2)$$

$$K^+p \rightarrow K^o n \pi^+ \pi^+, \quad K^o \rightarrow \pi^+ \pi^- \qquad \text{(208 events).} \qquad (3)$$

The cross-sections for these reactions, corrected for the invisible K^o decays, were determined by normalizing to the number of τ decays found in the same fiducial volumes. They are given in Table I, where for comparison, we also show the values obtained at $P_K = 1.96$ GeV/c[5)].

2. Production of Resonances

a) Let us first examine the events which fit reaction (1). If we plot a scatter diagram of the effective masses for the $(K^+\pi^-)$ and $(p\,\pi^+)$ systems, we see (Figure (1a)) that the $K^*(890)$ and $N^*(1238)$ are formed in abundance. Furthermore, there is an important clustering of events corresponding to the simultaneous formation of these two resonances.

If instead we consider a scatter diagram for the combination $(K^+\pi^+)$ and $(p\pi^-)$ (Figure (1b)), or for the combination $(\pi^+\pi^-)$ and (K^+p) (Figure 1c)), we find the events distributed throughout the plots in a rather uniform manner. No significant resonance peaks seem to be present in these combinations, as can also be seen on the corresponding effective mass distributions of Figure (2). Here we have also shown the four-body phase space predictions; the slight departure from the curves is due to the "reflection" of the resonance formation in the other channel.

To estimate the cross-sections for $K^*N\pi$, $N^*K\pi$ and simultaneous K^*N^* production, we analyse reaction (1) under the assumption that there are four

non-interfering contributions to its final state :

$$K^+p \rightarrow K^{*}N^{*}, \quad K^{*} \rightarrow K^+\pi^-, \quad N^{*} \rightarrow p\pi^+ ; \qquad (1a)$$

$$K^+p \rightarrow K^{*}p\pi^+, \quad K^{*} \rightarrow K^+\pi^- ; \qquad (1b)$$

$$K^+p \rightarrow N^{*}K^+\pi^-, \quad N^{*} \rightarrow p\pi^+ ; \qquad (1c)$$

$$K^+p \rightarrow K^+p\pi^+\pi^- \quad \text{(non-resonant)}. \qquad (1d)$$

The resonances present in (1a), (1b) and (1c) are described by p-wave relativistic Breit-Wigner distributions (see Appendix (A) for detailed formulae). The events corresponding to (1d) are assumed to be distributed according to their phase space. The combined density of events due to the contribution of all the above reactions is then written as :

$$L\,(M_{K\pi}, M_{p\pi}) = f_{K^{*}N^{*}}\, F_{K^{*}N^{*}} + f_{K^{*}}\, F_{K^{*}} + f_{N^{*}}\, F_{N^{*}} + (1 - f_{K^{*}N^{*}} - f_{K^{*}} - f_{N^{*}})\, F_{KN\pi\pi} \qquad (4)$$

where the f's are the fractions of events of each type and the F's are their effective mass distributions.

A likelihood analysis was made on the basis of this distribution (4) for the determination of the seven parameters : $M_{K^{*}}$, $M_{N^{*}}$, $\Gamma_{K^{*}}$, $\Gamma_{N^{*}}$, $f_{K^{*}N^{*}}$, $f_{K^{*}}$ and $f_{N^{*}}$. The maximum likelihood solution for these parameters is given in column 2 of Table II. The corresponding effective mass distributions agree well with the data as can be seen on Figures (3a) and (3b), where we have shown the projections of the scatter plot of Figure (1a) on the respective axes. It should be noticed that in the $K\pi$ effective mass spectrum, Figure (3a), there is no evidence for $\kappa(725)$ production as was found in the five-body final states, $KN\pi\pi\pi$, at the same energy[6].

b) An analysis similar to the one described in a) was performed for the events of reactions (2) and (3). With respect to reaction (1), there are differences to be noted here. Reaction (2) can yield a quasi two-body process in two different ways :

$$K^+p \rightarrow K^{*}N^{*}, \quad K^{*} \rightarrow K^0\pi^0, \quad N^{*} \rightarrow p\pi^+ ; \qquad (2a)$$

$$K^+p \rightarrow K^{*}N^{*}, \quad K^{*} \rightarrow K^0\pi^+, \quad N^{*} \rightarrow p\pi^0 \qquad (2b)$$

and reaction (3) with its two identical pions leads to a similar problem.

In the likelihood analysis of these reactions we have assumed that the presence of a resonance in one channel contributes as "phase space" when its decay products are introduced in the other ("wrong") combination. The scatter diagrams and their projections on the appropriate axes are shown on Figures (4), (5), (6) and (7); the combinations $(K^{o}p)$, $(\pi^{+}\pi^{o})$, $(K^{o}n)$ and $(\pi^{+}\pi^{+})$ do not exhibit any significant resonant peak and are not shown.

The maximum likelihood solutions for the parameters of these reactions are given in columns 3, 4 and 5 of Table II. In the case of reaction (3) no independent determination of the masses and widths of the K^{*} and the N^{*} was possible due to the small number of events involved; instead, a preset value for these quantities was used to determine the other parameters. We have independently calculated the maximum likelihood solutions for all reactions using preset values of the masses and widths of both resonances. Using the values obtained in the study of the three-body final state $K^{o}p\pi^{+}$ [4], we obtain, within statistics, the same values of the f-parameters.

c) Looking at the results on Table II, we notice that the values obtained in the different reactions for the masses of K^{*} and N^{*}, as well as their widths, agree reasonably well. We have verified that the values obtained for the mass of one of the resonances does not depend on the value found for the other. It is also worth noticing that the high percentage of $K^{*}N^{*}$ events ($52^{o}/o$) produced in reaction (1) makes this reaction particularly well suited for the study of the process $K^{+}p \rightarrow K^{*}N^{*}$. In contrast to this, one can see that for reactions (2) and (3) the simultaneous $K^{*}N^{*}$ production represents a much lower percentage of the total; the study of the $K^{*}N^{*}$ among these events will thereby be hindered by a larger background than that present in reaction (1).

From the results of the above analysis (a and b) we can calculate the cross-sections for all the double resonance channels. These cross-sections are connected, on the basis of isotopic spin invariance, by Clebsch-Gordan coefficients. For this, isotopic spin invariance is assumed for the production and decay of the resonances, together with the fact that the initial state has $I = 1$ and $I_{Z} = +1$. The comparison between the observed and predicted cross-sections is given in Table III.

The agreement is rather good and speaks well for the validity of the above analysis.

3. Analysis of the Decay Angular Distributions of the K^*N^* Events

We now examine in detail the decay angular distributions of the resonances formed in the reaction $K^+p \rightarrow K^*N^*$. We have seen that in all three reactions (1), (2), (3), a substantial fraction of the events proceed through the simultaneous formation of K^* and N^*. In order to select out these events, and at the same time reduce the relative background due to the other contributions, we have imposed the limits $0.86\ \text{GeV} \leqslant M_{K\pi} \leqslant 0.94\ \text{GeV}$ and $1.16\ \text{GeV} \leqslant M_{p\pi} \leqslant 1.29\ \text{GeV}$ on their effective masses. The effect of this selection is shown on Table IV[+]; here we see, for example, that the K^*N^* events represent 89°/o of the total number of reactions (1) which satisfy the above mass limits. As an additional purification of the sample considered we have further introduced a cut-off in the momentum transfer Δ^2 of reactions (1a), (2a) and (2b); only events with $\Delta^2 \leqslant 0.5\ (\text{GeV/c})^2$ were taken. This selection was suggested by the sharply peaked production angular distributions of these reactions (see Section 4, below); the events belonging to the background reactions are more likely to contribute to the high Δ^2 tail of the distributions. This was tested by examining the Δ^2 distributions for various regions outside the selected K^*N^* rectangular area of the scatter diagrams of Figures (1) and (4)[++].

The analysis of the decay distributions is most conveniently done in the rest frame of the resonance considered. We have used the coordinate system shown in Figure (8). For the K^* rest frame the z-axis was chosen as the direction of the incident K^+ (in the centre of mass system of the K^*) while for the N^* rest frame the z-axis was chosen as the direction of the target proton (in the centre of mass system of the N^*). For both resonances, the x-z plane is parallel to the production plane.

+) We have not included in Table IV the column corresponding to reaction (3) because here the combination of small statistics together with the large background makes this study less reliable.

++) When the four-body reaction is reduced to a three-body one (K^*, $N\pi$), the fractions of the reactions K^*, $p\pi$ and K^*N^* can be analysed using the method developed for the three-body case[4]. In this case it is allowed to make cuts in the production angle of the K^*. This cut still fills the whole Dalitz plot. In this way we arrive at the following fractions of K^*N^* events in the mass intervals used for the decay angular distributions : 97°/o for (1a), 93°/o for (2a), and 83°/o for (2b).

In general, the angular distribution of the K-meson from the decay of the K^{*} can be expressed in the form[7] :

$$W_{K^*}(\cos\theta,\varphi)\, d\cos\theta\, d\varphi = \frac{3}{4\pi}\Big[\rho_{0,0}\cos^2\theta + \frac{1}{2}(1-\rho_{0,0})\sin^2\theta - \rho_{1,-1}\sin^2\theta\cos 2\varphi - \sqrt{2}\,\mathrm{Re}\,\rho_{1,0}\sin 2\theta\cos\varphi\Big] d\cos\theta\, d\varphi \qquad (5)$$

from which we obtain the θ and φ distributions :

$$W_{K^*}(\cos\theta)\, d\cos\theta = \frac{3}{4}\Big[(1-\rho_{0,0}) + (3\rho_{0,0}-1)\cos^2\theta\Big] d\cos\theta \qquad (6a)$$

$$W_{K^*}(\varphi)\, d\varphi = \frac{1}{2\pi}\Big[1 - 2\rho_{1,-1} + 4\rho_{1,-1}\sin^2\varphi\Big] d\varphi \qquad (6b)$$

where θ and φ are the polar and azimuthal angles (Figure (8)) and the ρ's are elements of the K^{*} spin-space density matrix. Equation (5) is derived under the assumption that the K^{*} is a freely decaying particle of spin 1.

Similarly, the angular distribution of the proton from the decay of the N^{*} can be expressed as[7] :

$$W_{N^*}(\cos\theta,\varphi)\, d\cos\theta\, d\varphi = \frac{3}{4\pi}\Big[\rho_{3,3}\sin^2\theta + (\tfrac{1}{2}-\rho_{3,3})(\tfrac{1}{3}+\cos^2\theta) - \frac{2}{\sqrt{3}}\,\mathrm{Re}\,\rho_{3,1}\sin 2\theta\cos\varphi - \frac{2}{\sqrt{3}}\,\mathrm{Re}\,\rho_{3,-1}\sin^2\theta\cos 2\varphi\Big] d\cos\theta\, d\varphi \qquad (7)$$

from which we obtain :

$$W_{N^*}(\cos\theta)\, d\cos\theta = \frac{3}{4}\Big[\frac{1}{3}(1+4\rho_{3,3}) + (1-4\rho_{3,3})\cos^2\theta\Big] d\cos\theta \qquad (8a)$$

$$W_{N^*}(\varphi)\, d\varphi = \frac{1}{2\pi}\Big[1 - \frac{4}{\sqrt{3}}\,\mathrm{Re}\,\rho_{3,-1} + \frac{8}{\sqrt{3}}\,\mathrm{Re}\,\rho_{3,-1}\sin^2\varphi\Big] d\varphi \qquad (8b)$$

where the ρ parameters are elements of the N^{*} spin-space density matrix, and the N^{*} is assumed to be a freely decaying particle of spin 3/2.

The parameters $\rho_{0,0}$, $\rho_{1,-1}$, $\rho_{3,3}$ and $\mathrm{Re}\,\rho_{3,-1}$ were determined by a maximum likelihood analysis of the data based on equations (5) and (7). The parameters $\mathrm{Re}\,\rho_{1,0}$ and $\mathrm{Re}\,\rho_{3,1}$ were calculated by means of the equations

$$\mathrm{Re}\,\rho_{1,0} = -\frac{5}{4\sqrt{2}}\,\langle \sin 2\theta\cos\varphi\rangle \qquad (9)$$

$$\mathrm{Re}\,\rho_{3,1} = -\frac{5\sqrt{3}}{8}\,\langle \sin 2\theta\cos\varphi\rangle . \qquad (10)$$

The values thus obtained, together with their allowed range, are given in Table V.

A comparison between the ρ parameters for the different reactions of Table V shows that, within the statistical errors, there are no significant differences. In the case of reaction (1a) we have calculated corrections to the ρ parameters to account for the presence of the "non-$K^{*}N^{*}$ events" by considering events in the regions surrounding the rectangular area selected for our samples. These corrections turned out to be, at most, equal to the statistical errors and were neglected. The θ and φ decay angular distributions for the K^{*} and N^{*} from reaction (1a) are shown in Figure (9) together with the best fits using the ρ values of Table V. Similar decay angular distributions were obtained for the K^{*} and N^{*} from reactions (2a) and (2b) and are not shown.

4. Production Mechanisms of $K^{*}N^{*}$

If we look at the c.m. production angular distributions for the $K^{*}N^{*}$ events (Figure (10)), we see that the K^{*}'s are very sharply peaked in the forward direction with respect to the incident K^{+} (and, of course, the N^{*}'s are peaked in the backward direction). This suggests peripheralism as the production mechanism and the use of a one-meson exchange model for the interpretation of the data. The simplest diagram corresponding to this phenomenon is shown on Figure (11).

a) One-meson exchange model

For the K^{*} vertex, the situation is identical to the one encountered in the study of the three-body reaction $K^{o}p\pi^{+}$; we refer to that paper for a full account on the possible exchanged particles at this vertex[4]. We only recall that in the framework of a simple one-meson exchange model, a single π-exchange corresponds to a decay angular distribution (6a) proportional to $\cos^{2}\theta$ (i.e. $\rho_{0,0}= 1$); a vector meson exchange, on the other hand, leads to a decay angular distribution (6a) proportional to $\sin^{2}\theta$ (i.e. $\rho_{0,0}= 0$). The parameter $\rho_{0,0}$ can therefore be interpreted as the fraction of the events which proceed by way of pion exchange. In the case of pion exchange the azimuthal angular distribution φ is isotropic ($\rho_{1,-1}= 0$) whereas it is in general non-isotropic for vector meson exchange (the φ distribution is in fact identical to the so-called Treiman-Yang angular distribution[8),9)]).

As can be seen in Table V, $\rho_{0,0}$ for reaction (1a) is equal to 0.76 ± 0.05, indicating that a large fraction of the events - though not all - can be interpreted as proceeding via the exchange of a single pion+). The parameter Re $\rho_{1,0}$ is equal to -0.13 ± 0.02 which is significantly different from 0, the value it should have in our simple one-meson exchange model[7] (pseudoscalar and/or vector meson exchange).

For the N^* vertex, it is easy to show that when there is pion exchange the polar angular distribution is predicted to be $1 + 3\cos^2\theta$ and the azimuthal distribution is isotropic. This corresponds to $\rho_{3,3} = \text{Re}\ \rho_{3,-1} = \text{Re}\ \rho_{3,1} = 0$. If, on the other hand, there is vector meson exchange, it is reasonable to expect it to proceed by way of the ρ-meson exchange mechanism of Stodolsky and Sakurai[13], which seems to describe the vector meson exchange observed in the reaction $K^+p \rightarrow K^0N^{*++}$ [4]. This model predicts $\rho_{3,3} = 0.375$, Re $\rho_{3,-1} = 0.216$ and Re $\rho_{3,1} = 0$. Since the measured value of $\rho_{3,3}$ is nearly zero (0.01 ± 0.04), these data again indicate a predominance of pion exchange. At the same time, the significantly non-zero value of Re $\rho_{3,1}$ (0.07 ± 0.02) provides another demonstration that the simple exchange model is not fully adequate.

It should also be noticed that the non-pion part of our one-meson exchange would require the exchange of a vector meson. Recent results[10),11] indicate that in the reactions $K^+n \rightarrow K^{*0}p$ and $K^-p \rightarrow \bar{K}^{*0}n$ the exchanged particle (which has to be charged, as in reactions (1a) and (2a)) appears predominantly to be a 0^- particle. These results are in agreement with the Bronzan and Low assignment of a quantum number for amplitude parity[12] according to which a $K\rho K^*$ vertex is forbidden. We also notice that at the N^* vertex the exchange of a T = 0 vector meson is forbidden by isotopic spin conservation. Hence, ω-exchange is forbidden and since ρ-exchange seems also to be excluded, the vector meson part of the simple one-meson exchange becomes difficult to interpret.

The validity of this one-meson exchange model may also be tested by a comparison between the theoretical prediction and the experimental values for the production angular distribution. An attempt at such a comparison is made on

---

+) We have estimated from the published data at 1.96 GeV/c[5] and for events corresponding to the same cut in the Δ^2 distribution that $\rho_{0,0} = 0.85 \pm 0.1$ which is again in agreement with a predominance of pion exchange.

Figure (10a) where we show the distribution of the c.m. production angle for the K^{*} of reaction (1a). The dashed curve represents the prediction of the simple one-meson exchange model on the assumption that only pion exchange contributes. It corresponds to the following expression[14] :

$$\frac{d\sigma}{d\Omega}\,(\mathrm{mb/ster}) = C\,\frac{P_{K^{*}}}{P_{K^{+}}}\times\frac{1}{E^{2}_{tot}}\times\frac{1}{6M^{2}_{K^{*}}M^{2}_{N^{*}}}\times\frac{1}{(M_{N^{*}}+M_{P})^{2}-m^{2}_{\pi}}$$

$$\times\frac{g^{2}_{K^{*}}}{4\pi}\times\frac{g^{2}_{N^{*}}}{4\pi}\times\frac{1}{(\Delta^{2}+m^{2}_{\pi})^{2}}\times\left[\Delta^{2}+(M_{K^{*}}+M_{K})^{2}\right]\times\left[\Delta^{2}+(M_{K^{*}}-M_{K})^{2}\right]$$

$$\times\left[\Delta^{2}+(M_{N^{*}}+M_{p})^{2}\right]^{2}\times\left[\Delta^{2}+(M_{N^{*}}-M_{p})^{2}\right]. \qquad (11)$$

In this expression, $\frac{g^{2}_{K^{*}}}{4\pi} = \frac{2\,\Gamma_{K^{*}}\,M^{2}_{K^{*}}}{3P^{3}_{N,N^{*}}} = 1.0$ (the coefficient 2/3 accounts for the particular decay mode considered), $\frac{g^{2}_{N^{*}}}{4\pi} = \frac{3\,\Gamma_{N^{*}}\,M^{2}_{N^{*}}}{2P^{3}_{N,N^{*}}} = 26$, with $\Gamma_{N^{*}} = 140$ MeV. $P_{A,B}$ represents the momentum of particle A in the rest frame B, $P_{K^{+}}$ and $P_{K^{*}}$ are the c.m. momenta of the incident K^{+} and the outgoing K^{*}, respectively, and $C = (\hbar c)^{2} = 0.391$ GeV^{2} mb.

From the dashed curve on Figure (10a) we see that the model predicts a differential cross-section which strongly differs from the experimental one, both in shape and absolute value +).

In order to get a good agreement with the experimental distribution one usually multiplies the theoretical distribution (11) by a form factor $F^{2}(\Delta^{2})$. This form factor can take a variety of equally suitable expressions. The solid curve on Figure (10a) is the one-pion exchange distribution multiplied by the form factor $F^{2}(\Delta^{2}) = \left[\frac{\alpha^{2}-m^{2}_{\pi}}{\alpha^{2}+\Delta^{2}}\right]^{2}$ with $\alpha^{2} = 0.165$ (GeV/c)^{2} as derived from the data at 1.96 GeV/c[14]. The agreement with the experimental data is not as good here as it was at 1.96 GeV/c. Even though it is conceivable that an appropriate form factor could be found to satisfy our data, the introduction of an energy-dependent form factor is unattractive. This fact, in addition to the

+) The same remarks were already made at 1.96 GeV/c (Ref. (5)).

non-zero value obtained for the parameter Re $\rho_{1,0}$, clearly indicates that the simple one-meson exchange model cannot be considered as a satisfactory explanation of the data.

b) Modified one-meson exchange model

From the considerations given in a) it appears that for a complete understanding of the production mechanism and of the decay correlation of the K^*N^* reaction, it may be necessary to modify the simple one-meson exchange model. In particular, an attempt can be made at explaining the highly peaked production angular distribution without the use of ad-hoc form factors. This was done by Gottfried, Jackson, Keyser and Svensson[15]; they consider a model+) in which absorption effects due to competing processes are taken into account. The predictions of such a model are in pretty good agreement with the experimental facts in the case of the reactions $K^+p \rightarrow K^{*+}p$ and $K^+p \rightarrow N^{*}K^o$ at 3 GeV/c[4]. It is therefore tempting to try this model in the present case. In the calculations of the G.J.K.S. model[15], only π-exchange is considered, for which the coupling constants at both vertices are known. In this model the amount of absorption in the initial state was deduced from the K^+p elastic scattering data[16] and from it an estimate was made for the absorption in the final state. This latter estimate does not critically affect the final results.

To allow a comparison between the experimental results and the theoretical predictions, we have determined the ρ parameters for the reaction (1a) as a function of the four-momentum transfer. The Δ^2 intervals chosen and the values of the parameters are given in Table VI and shown in Figure (12). On the same figure we have also shown the predictions obtained so far by the G.J.K.S. model[15]. We see that the general trend for the parameter $\rho_{0,0}$ is correctly described by the model. In particular, there is no necessity of invoking vector meson exchange in order to explain the value of $\rho_{0,0}$ less than one. The agreement for the other parameters is not as good but still acceptable. Moreover, the model predicts values of Re $\rho_{1,0}$ different from zero as is observed experimentally.

+) Hereafter referred to as the G.J.K.S. model.

On Figure (10a) we have represented by crosses the values of the differential production cross-section predicted by the G.J.K.S. model. We see that the angular dependence of the cross-section is here in much better agreement with the experimental values than is the prediction of the unmodified single one-meson exchange model (dashed curve). On the other hand, the absolute value of the cross-section is still off by a factor of approximately 3[+]. We can, therefore, consider the G.J.K.S. model as a fruitful, although not completely successful, attempt at explaining the data[17].

Conclusion

In the final states $K^+p \rightarrow KN\pi\pi$ at 3 GeV/c, the double resonance reaction K^*N^* occurs in large proportion. It is found that the K^* is sharply peaked in the forward direction in the c.m. system, suggesting a peripheral process. The decay angular distributions for this reaction were studied in terms of the density matrix elements. The main result of this study is that, within the framework of a simple one-meson exchange model, the reaction proceeds predominantly through the exchange of a pion. In contrast to this, vector-meson exchange plays a dominant role in the reactions $K^+p \rightarrow K^{*+}p$ and $K^+p \rightarrow N^{*++}K^o$ at the same energy[4].

In the simple one-meson exchange model some vector-meson exchange is needed for the interpretation of the decay angular distributions, but ω-exchange is forbidden (by isotopic spin conservation) and ρ-exchange also appears to be suppressed[10),11),12]. More than that, it should be emphasized that the model cannot account for the non-zero value of the parameter Re $\rho_{1,0}$.

Another drawback of the simple one-meson exchange model is that it is unable to fit the K^*N^* production cross-section without the use of a drastic ad-hoc form factor similar to the one needed at 1.96 GeV/c[5].

A modified one-meson exchange model which takes into account the absorption due to competing processes was developed by Gottfried, Jackson, Keyser and Svensson[15]. Their theory does not explain the magnitude of the cross-sections, but it succeeds in accounting, with a minimum of assumptions, for both the production angular distribution and the decay correlations.

+) Some admixture of vector-meson exchange might succeed in reducing the predicted cross-section but as mentioned in a) this is counter-indicated by the experimental results[10),11)].

Acknowledgments

We have profited from many discussions with Professors J.D. Jackson and K. Gottfried, and Drs. H. Pilkuhn and B. Svensson. Dr. R. Böck has been very helpful in the development of many of the computer programs that we used. Our thanks are due to the crew of the 81 cm hydrogen bubble chamber, to the staff of the CERN proton synchrotron and to our scanning staff. We are grateful for the support given to us by Professor Ch. Peyrou.

Appendix A

The distribution function over the triangle, Figure (1a), for the reaction $K^+p \rightarrow K^{*}p\pi^+$ (1b), is taken to be[9] :

$$F_{K^*}(M_{K\pi}, M_{p\pi})\, dM_{K\pi}\, dM_{p\pi} = \left[\frac{\Gamma}{(M^2_{K\pi} - M^2_{K^*})^2 + \Gamma^2 M^2_{K^*}} \frac{M_{K\pi}}{q_{K\pi}} \right] \times q_{p,\pi} \times q_{K,\pi} \times q_{K\pi,\, p\pi} \times dM_{K\pi} \times dM_{p\pi} \qquad (1A)$$

$$\text{with } \Gamma = \Gamma_{K^*} \times \frac{q^3_{K,\pi}}{q^3_{K,\pi}(M_{K^*})} \times \frac{M_{K^*}}{M_{K\pi}}$$

where M_{K^*} and Γ_{K^*} are the intrinsic mass and width of the K^*, $q_{K,\pi}$ and $q_{p,\pi}$ are respectively the relative momenta between the K and π in the rest system for $M_{K\pi}$ and between the p and π in the rest system for $M_{p\pi}$, and where $q_{K\pi,p\pi}$ is the relative momentum between the $(K\pi)$ and $(p\pi)$ mass combinations in the c.m. system.

The relativistic Breit-Signer distribution used $\Gamma / [(M^2_{K\pi} - M^2_{K^*})^2 + \Gamma^2 M^2_{K^*}]$ contains only one power of Γ in the numerator because the resonance appears only in the final state and not in the initial state of the reaction. The formula for the width Γ is based on the assumption that at the decay of the resonance the interaction radius is small compared to $\hbar c/\Gamma$. The $q^3_{K,\pi}$ is the consequence of a p-wave decay, i.e. the orbital angular momentul $\ell = 1$ for the decay. The term $q^3_{K,\pi}(M_{K^*})$ corresponds to the value of $q^3_{K,\pi}$ when $M_{K\pi} = M_{K^*}$. The $M_{K\pi}$ term is a factor appropriate for the decay of a vector meson (1^-) into two speudo-scalar mesons.

The distribution function over the triangle, Figure (1a), for the reaction $K^+p \rightarrow N^{*}K^+\pi^-$ (1c) is taken to be[9] :

$$F_{N^*}(M_{K\pi}, M_{p\pi})\, dM_{K\pi}\, dM_{p\pi} = \left[\frac{\Gamma}{(M^2_{p\pi} - M^2_{N^*})^2 + \Gamma^2 M^2_{N^*}} \frac{M_{p\pi}}{q_{p,\pi}} \right] \times q_{p,\pi} \times q_{K,\pi} \times q_{K\pi,\, p\pi} \times dM_{p\pi} \times dM_{K\pi} \qquad (2A)$$

where $\Gamma = \Gamma_{N^*} \times \frac{q^3_{p,\pi}}{q^3_{p,\pi}(M_{N^*})} \times \left[\frac{(M_{p\pi} + M_p)^2 - M_\pi^2}{M^2_{p\pi}} \times \frac{M^2_{N^*}}{(M_{N^*} + M_p)^2 - M_\pi^2} \right]$.

Where M_π and M_p are the pion and proton masses all other quantities are defined analogously to those in the formula for K^*. The factor in brackets in the expression for Γ is the result found from first order perturbation theory for N^* decay.

The distribution function for the reaction $K^+p \rightarrow K^*N^*$ (1a) is written as the product of the distributions (1A) and (2A) :

$$F_{K^*N^*}\, dM_{K\pi}\, dK_{p\pi} = [(1A)] \times [(2A)] \times q_{p,\pi} \times q_{K,\pi} \times q_{K\pi,p\pi} \times dM_{p\pi} \times dM_{K\pi} \qquad (3A)$$

where the quantities in square brackets in (3A) are equal to the corresponding quantities in the square brackets of (1A) and (2A).

The distribution function for the reaction $K^+p \rightarrow K^+p\pi^+\pi^-$ (non-resonant) (1d) is taken to be :

$$F_{KN\pi\pi}\, dM_{K\pi}\, dM_{p\pi} = q_{p,\pi} \times q_{K,\pi} \times q_{K\pi,p\pi} \times dM_{p\pi} \times dM_{K\pi} \quad . \qquad (4A)$$

The distribution functions (1A) through (4A) have to be normalized before being used in the likelihood function (4). This was done by dividing the above-mentioned functions by their integral over the triangle (Figure (1a)).

Our results (column 2 of Table II) give values of $M_{N^*} = 1220 \pm 6$ MeV and $\Gamma_{N^*} = 125 \pm 30$ MeV for the mass and width of the N^{*++} of reaction (1a). These can be compared, for example, to the values of $M_{N^*} = 1232 \pm 6$ MeV and $\Gamma_{N^*} = 125 \pm 20$ MeV, obtained in a previous study of the three-body final state $K^0p\pi^+$ at 3 GeV/c[4]. In the latter case a dynamic factor q_K^3 (q_K = momentum of the K^0 in the c.m. system), appropriate when the resonance is produced via the exchange of a vector meson, was introduced in the formula for the N^* density distribution. Here, no such model-dependent term was used, however; even if it were it would not be enough to account for the difference in the values of M_{N^*}. Similarly, the values of 896 ± 3 MeV and 49 ± 4 MeV for the mass and width of the K^{*0} can be compared to the corresponding values obtained for the K^{*+} in the $K^0p\pi^+$ final state[4], i.e. 891 ± 3 MeV and 47 ± 4 MeV.

References

1) M. Ferro-Luzzi, R. George, Y. Goldschmidt-Clermont, V.P. Henri, B. Jongejans, D.W.G. Leith, G.R. Lynch, F. Muller and J.-M. Perreau, Proceedings of the Sienna International Conference on Elementary Particles, Vol. 1, 189 (1963).

2) J. Goldberg and J.-M. Perreau, "Un faisceau d'usage général à deux étages de séparation électrostatique au PS" (CERN 63-12, April 9, 1963).

3) G.R. Lynch, M. Ferro-Luzzi, R. George, Y. Goldschmidt-Clermont, V.P. Henri, B. Jongejans, D.W.G. Leith, F. Muller and J.-M. Perreau, Physics Letters 9, 359 (1964).

4) M. Ferro-Luzzi, R. George, Y. Goldschmidt-Clermont, V.P. Henri, B. Jongejans, D.W.G. Leith, G.R. Lynch, F. Muller and J.-M. Perreau, "The reaction $K^+p \rightarrow K^0p\pi^+$ at 3 GeV/c", to be published in Nuovo Cimento.

5) G. Goldhaber, W. Chinowsky, S. Goldhaber, W. Lee and T. O'Halloran, Physics Letters 6, 62 (1963).
Similar conclusions can be deduced from preliminary results at 2.26 GeV/c - see R. Kraemer, L. Madansky, I. Miller, A. Pevsner, C. Richardson, R. Singh, R. Zdanis, Proceedings Athens Topical Conference on Recently Discovered Resonant Particles (1963).

6) M. Ferro-Luzzi, R. George, Y. Goldschmidt-Clermont, V.P. Henri, B. Jongejans, D.W.G. Leith, G.R. Lynch, F. Muller and J.-M. Perreau, Physics Letters 12, 255 (1964).

7) K. Gottfried and J.D. Jackson, Physics Letters 8, 144 (1964), and Nuovo Cimento 33, 309 (1964).

8) S.B. Treiman and C.N. Yang, Phys.Rev.Letters 8, 140 (1962).

9) J.D. Jackson, Nuovo Cimento 34, 1644 (1964).

10) S. Goldhaber, I. Butterworth, G. Goldhaber, A.A. Hirata, J.A. Kadyk, T.A. O'Halloran, B.C. Shen and G.H. Trilling, "K^+d interactions at 2.3 GeV/c", Paper presented at the 1964 International Conference on High Energy Physics at Dubna.

PS/4801/mhg

11) R. Barloutaud, A. Lévèque, C. Louedec, J. Meyer, P. Schlein, A. Verglas, J. Badier, M. Demoulin, J. Goldberg, B.P. Gregory, P. Krejbich, C. Pelletier, M. Ville, E.S. Gelsema, J. Hoogland, J.C. Kluyver and A.G. Tenner, Physics Letters 12, 352 (1964).

12) J.B. Bronzan and F.E. Low, Phys.Rev.Letters 12, 522 (1964).

13) L. Stodolsky and J.J. Sakurai, Phys.Rev.Letters 11, 90 (1963).

14) J.D. Jackson and H. Pilkuhn, Nuovo Cimento 33, 906 (1964).

15) K. Gottfried, J.D. Jackson, R. Keyser and B. Svensson, to be published; see also K. Gottfried and J.D. Jackson, Nuovo Cimento 34, 753 (1964).

16) J. Debaisieux, F. Grard, J. Heughebaert, L. Pape, R. Windmolders, M. Ferro-Luzzi, R. George, Y. Goldschmidt-Clermont, V.P. Henri, B. Jongejans, D.W.G. Leith, G.R. Lynch, F. Muller, J.-M. Perreau, G. Otter and P. Sälström, "K^+p elastic scattering at 3.0 and 3.5 GeV/c", Paper presented at the 1964 International Conference on High Energy Physics at Dubna.

17) J.D. Jackson, "Peripheral production and decay correlations of resonances", to be published in the Reviews of Modern Physics.

Table I

Comparison between the cross-sections, corrected for the invisible K^o decays, for reactions (1), (2) and (3) at 2.97 GeV/c and 1.96 GeV/c.

Reaction	P_K = 2.97 GeV/c σ (mb)	P_K = 1.96 GeV/c[a] σ (mb)
$K^+ p \pi^+ \pi^-$ (1)	2.3 ± 0.3	1.7 ± 0.2
$K^o p \pi^+ \pi^o$ (2)	2.1 ± 0.3	1.3 ± 0.2
$K^o n \pi^+ \pi^+$ (3)	0.6 ± 0.2	0.33 ± 0.1

a) Reference 5)

Table II

Parameters of the maximum likelihood solution of equation (4) for reactions (1), (2), (3).
Masses and widths in MeV, fractions in °/o.

Parameter \ Reaction	$K^+ p \pi^+ \pi^-$ (1)	$K^0 p \pi^+ \pi^0$ (2)		$K^0 n \pi^+ \pi^+$ (3)
	$K^* \to K^+\pi^-$; $N^* \to p\pi^+$	$K^* \to K^0\pi^0$; $N^* \to p\pi^+$	$K^* \to K^0\pi^+$; $N^* \to p\pi^0$	$K^* \to K^0\pi^+$; $N^* \to n\pi^+$
M_{K^*}	896 ± 3	893 ± 4	895 ± 3	(896, input)
Γ_{K^*}	49 ± 4	57 ± 9	50 ± 10	(49, input)
M_{N^*}	1220 ± 6	1230 ± 8	1240 ± 8	(1220, input)
Γ_{N^*}	125 ± 30	175 ± 30	125 ± 25	(125, input)
$f_{K^*N^*}$	52 ± 3	22 ± 2	9 ± 1	18 ± 8
f_{K^*}	6 ± 2	8 ± 3	15 ± 3	30 ± 6
f_{N^*}	15 ± 3	21 ± 3	1^{+5}_{-1}	20 ± 8
$f_{KN\pi\pi}$	27 ± 3	← 24 ± 3 →		32 ± 8

Table III

Observed and predicted (by Clebsch-Gordan coefficients) cross-sections for the various charge states of the reaction $K^+p \rightarrow K^* N^*$.

$K^* N^*$ Charge state	Observed (a) Cross-sections (mb)	Observed (a) Percentages	Predicted (a) Percentages
$(K^+ \pi^-)(p \pi^+)$	$1.2 \pm .2$	61 ± 10	55
$(K^o \pi^o)(p \pi^+)$	$0.46 \pm .09$	24 ± 5	27
$(K^o \pi^+)(p \pi^o)$	0.18 ± 0.04	9 ± 2	12
$(K^o \pi^+)(n \pi^+)$	0.11 ± 0.05	6 ± 3	6

(a) Corrected for invisible K^o decays.

Table IV

Contributions (in %) of $K^{*}N^{*}$, $K^{*}N\pi$, $N^{*}K\pi$ and $KN\pi\pi$ for events with effective masses 0.86 GeV $\leqslant M_{K\pi} \leqslant$ 0.94 GeV and 1.16 GeV $\leqslant M_{p\pi} \leqslant$ 1.29 GeV in reactions (1) and (2).

Reaction / Percentage of	$K^+p\pi^+\pi^-$ (1)	$K^0p\pi^+\pi^0$ (2)	
	$K^{*}\to K^+\pi^-$, $N^{*}\to p\pi^+$ (1a)	$K^{*}\to K^0\pi^0$, $N^{*}\to p\pi^+$ (2a)	$K^{*}\to K^0\pi^+$, $N^{*}\to p\pi^0$ (2b)
$K^{*}\ N^{*}$	89	67	51
$K^{*}\ N\ \pi$	3	7	20
$N^{*}\ K\ \pi$	5	13	2
$N\ K\ \pi\ \pi$	3	13	27

Table V

Decay parameters for the $K^{*}N^{*}$ reaction. Selected events with effective masses $0.86\ \text{GeV} \leqslant M_{K\pi} \leqslant 0.94\ \text{GeV}$ and $1.16\ \text{GeV} \leqslant M_{p\pi} \leqslant 1.29\ \text{GeV}$ and momentum transfer $\Delta^2 \leqslant 0.5\ (\text{GeV/c})^2$.

Parameter	Range	$K^+p\pi^+\pi^-$ (1)	$K^0p\pi^+\pi^0$ (2)	
		$K^{*}\to K^+\pi^-$, $N^{*}\to p\pi^+$ (1a)	$K^{*}\to K^0\pi^0$, $N^{*}\to p\pi^+$ (2a)	$K^{*}\to K^0\pi^+$, $N^{*}\to p\pi^0$ (2b)
$\rho_{0,0}$	0, 1	0.76 ± 0.05	0.64 ± 0.09	0.70 ± 0.11
$\rho_{1,-1}$	-1/2, 1/2	-0.03 ± 0.03	0.12 ± 0.09	-0.03 ± 0.10
Re $\rho_{1,0}$ [a]	$-1/2\sqrt{2}$, $1/2\sqrt{2}$	-0.13 ± 0.02	-0.13 ± 0.05	-0.15 ± 0.05
$\rho_{3,3}$	0, 1/2	0.01 ± 0.04	0.09 ± 0.05	0.20 ± 0.07
Re $\rho_{3,-1}$	$-\sqrt{3}/4$, $\sqrt{3}/4$	-0.035 ± 0.035	0.07 ± 0.08	0.00 ± 0.08
Re $\rho_{3,1}$ [a]	$-\sqrt{3}/4$, $\sqrt{3}/4$	0.07 ± 0.02	0.03 ± 0.06	0.04 ± 0.06

a) The sign of the parameters Re $\rho_{1,0}$ and Re $\rho_{3,1}$ is determined by the choice of the normal to the production plane (Figure (8)).

Table VI

Decay parameters for the reaction $K^+p \to K^{*}N^{*}$ ($K^{*} \to K^+\pi^-$, $N^{*} \to p\pi^+$) as a function of the four-momentum transfer Δ^2. Selected events with mass intevals 0.86 GeV $\leqslant M_{K\pi} \leqslant$ 0.94 GeV and 1.16 GeV $\leqslant M_{p\pi} \leqslant$ 1.29 GeV.

Δ^2 Interval $(GeV/c)^2$	$\rho_{0,0}$	$\rho_{1,-1}$	Re $\rho_{1,0}$	$\rho_{3,3}$	Re $\rho_{3,-1}$	Re $\rho_{3,1}$
$0.11 \leqslant \Delta^2 \leqslant 0.16$	0.86 ± 0.08	0.07 ± 0.07	-0.14 ± 0.04	-0.01 ± 0.05	0.02 ± 0.06	0.03 ± 0.05
$0.16 \leqslant \Delta^2 \leqslant 0.24$	0.82 ± 0.07	-0.03 ± 0.09	-0.18 ± 0.04	0.09 ± 0.07	-0.10 ± 0.07	0.14 ± 0.05
$0.24 \leqslant \Delta^2 \leqslant 0.42$	0.60 ± 0.10	-0.11 ± 0.10	-0.06 ± 0.04	-0.02 ± 0.08	-0.07 ± 0.07	0.07 ± 0.05
$0.42 \leqslant \Delta^2 \leqslant 1$	0.45 ± 0.15	0.21 ± 0.10	-0.15 ± 0.07	0.20 ± 0.08	0.06 ± 0.09	0.03 ± 0.08

Figure Captions

Fig. 1 Scatter diagrams of the effective masses for the two-particle systems of the reaction $K^+p \rightarrow K^+p\pi^+\pi^-$. The triangles correspond to the kinematical limits.

Fig. 2 Effective mass spectra for the events shown in Figures (1b) and (1c). The solid curves represent phase space.

Fig. 3 $(K^+\pi^-)$ and $(p\pi^+)$ effective mass spectra for the events shown in Figure (1a). The five curves represent respectively the normalized distribution function (Equation (4), called TOTAL) and its four terms with the parameters of Table II, Column (2). The expressions for the F's are given in Appendix A.

Fig. 4 Scatter diagrams of the two $(K\pi)$ versus $(p\pi)$ effective masses contributions for the reaction $K^+p \rightarrow K^0p\pi^+\pi^0$.

Fig. 5 Effective mass spectra for the events shown in Figures (4a) and (4b). The curves have the same meaning as in Figure (3) and the notations are identical.

Fig. 6 Scatter diagram of the $(K\pi)$ versus $(n\pi)$ effective masses for the reaction $K^+p \rightarrow K^0n\pi^+\pi^+$. Each event is plotted twice because of the presence of two identical pions.

Fig. 7 Effective mass spectra for the events shown in Fig. (6). The curves have the same meaning as in Figure (3) and the notations are identical.

Fig. 8 Coordinate system used in the analysis of the decay angular distributions. The notation $\vec{P}_{A,B}$ represents the momentum of particle A in the rest frame of B. cm. refers to the overall centre of mass system. $\vec{P}_{K^+_i}$ and $\vec{P}_{K_f}$ are respectively the momenta of the incident K^+ and of the outgoing K from the decay of the K^*. $\vec{P}_{p_i}$ and $\vec{P}_{p_f}$ are respectively the momenta of the target proton and of the outgoing proton from the decay of the N^*. The XZ plane is parallel to the production plane. Y is the chosen direction for the normal to the production plane.

Fig. 9 Polar ($\cos\theta$) and azimuthal(ϕ) angular distribution for the events of the reaction $K^+p \rightarrow K^{*}N^{*}$, $K^{*} \rightarrow K^+\pi^-$, $N^{*} \rightarrow p\pi^+$ for events with effective masses $0.86\ \text{GeV} \leqslant M_{K\pi} \leqslant 0.94\ \text{GeV}$ and $1.16\ \text{GeV} \leqslant M_{p\pi} \leqslant 1.29\ \text{GeV}$ and momentum transfer $\Delta^2 \leqslant 0.5\ (\text{GeV/c})^2$. Figures (a) and (b) are for the K^{*} and Figures (c) and (d) for the N^{*}. The solid curves are best fits using the ρ-parameters of Table V, Column 3 and Equations (6a), (6b); (8a) and (8b).

Fig. 10 K^{*} production angular distributions for events with effective masses $0.86\ \text{GeV} \leqslant M_{K\pi} \leqslant 0.94\ \text{GeV}$ and $1.16\ \text{GeV} \leqslant M_{p\pi} \leqslant 1.29\ \text{GeV}$. Figure (a) corresponds to the reaction $K^+p \rightarrow K^{*}N^{*}$, $K^{*} \rightarrow K^+\pi^-$, $N^{*} \rightarrow p\pi^+$. The dashed curve at the top of the figure represents the prediction of the simple one-meson exchange model on the assumption that only pion exchange contributes. The solid curve is the one-pion exchange distribution multiplied by a form factor $F^2(\Delta^2) = \left(\frac{\alpha^2 - m_\pi^2}{\alpha^2 + \Delta^2}\right)^2$ with $\alpha^2 = 0.165\ (\text{GeV/c})^2$ as derived from the data at 1.96 GeV/c[14]. The curve with crosses shows the values of the cross-section as predicted by the modified one-meson exchange model, taking into account absorption effects[15].
Figure (b) corresponds to the reaction $K^+p \rightarrow K^{*}N^{*}$, $K^{*} \rightarrow K^0\pi^0$, $N^{*} \rightarrow p\pi^+$, and Figure (c) to $K^+p \rightarrow K^{*}N^{*}$, $K^{*} \rightarrow K^0\pi^+$, $N^{*} \rightarrow p\pi^0$ for events with the same effective mass intervals as in Figure (a).

Fig. 11 Feynman diagram for the reaction $K^+p \rightarrow K^{*}N^{*}$.

Fig. 12 ρ-parameters for the reaction $K^+p \rightarrow K^{*}N^{*}$, $K^{*} \rightarrow K^+\pi^-$, $N^{*} \rightarrow p\pi^+$, for events with effective masses $0.86\ \text{GeV} \leqslant M_{K\pi} \leqslant 0.94\ \text{GeV}$ and $1.16\ \text{GeV} \leqslant M_{p\pi} \leqslant 1.29\ \text{GeV}$, as a function of various momentum transfer intervals. The Δ^2 intervals chosen (Table VI) are indicated by horizontal arrows. The ρ values, plotted at the centre of a given Δ^2 interval, are averages over the Δ^2 region. The curves are the predictions of the G.J.K.S. model.

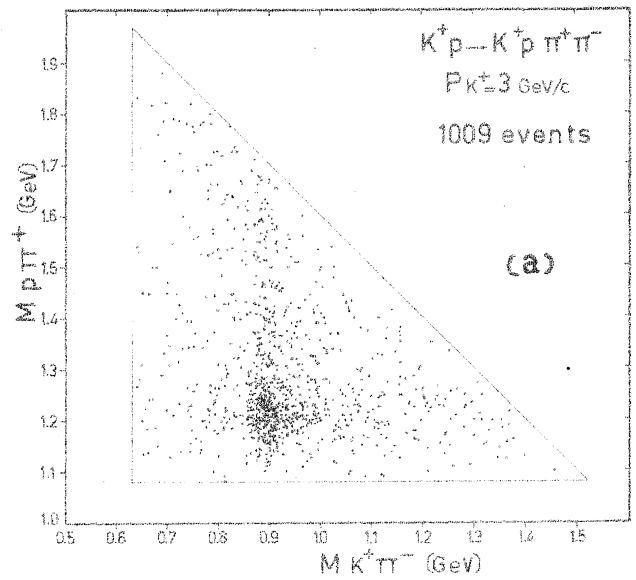

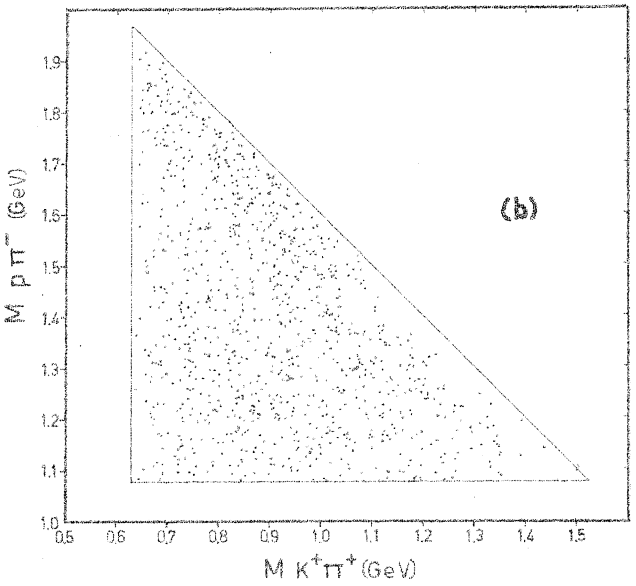

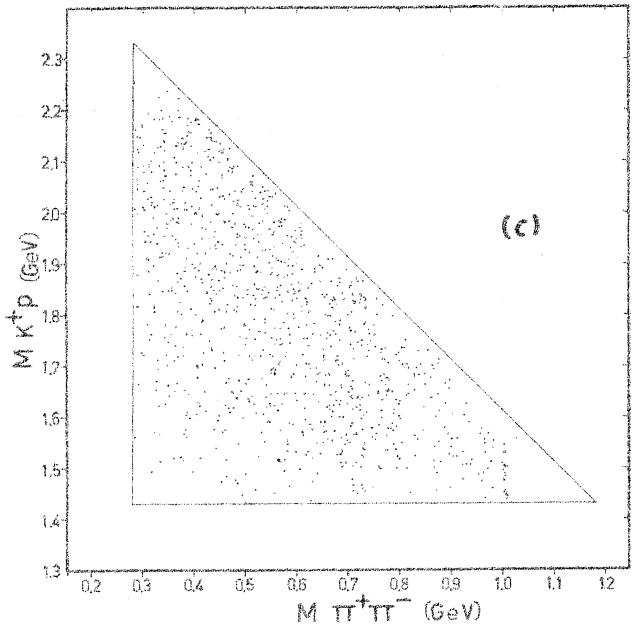

PS/4801/mhg

FIG 1.

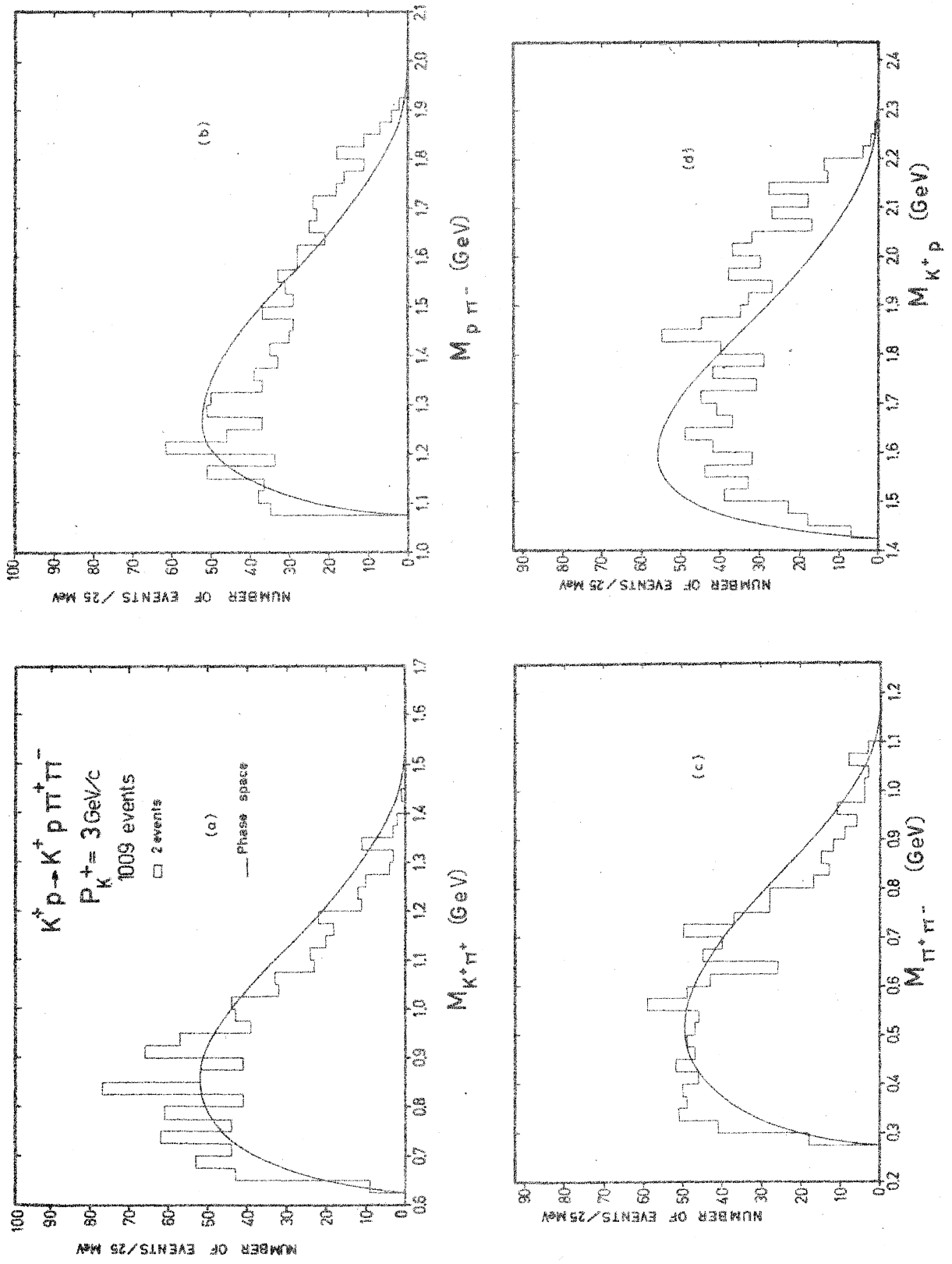

FIG. 2

DIR 22300

PS/4801/mkg

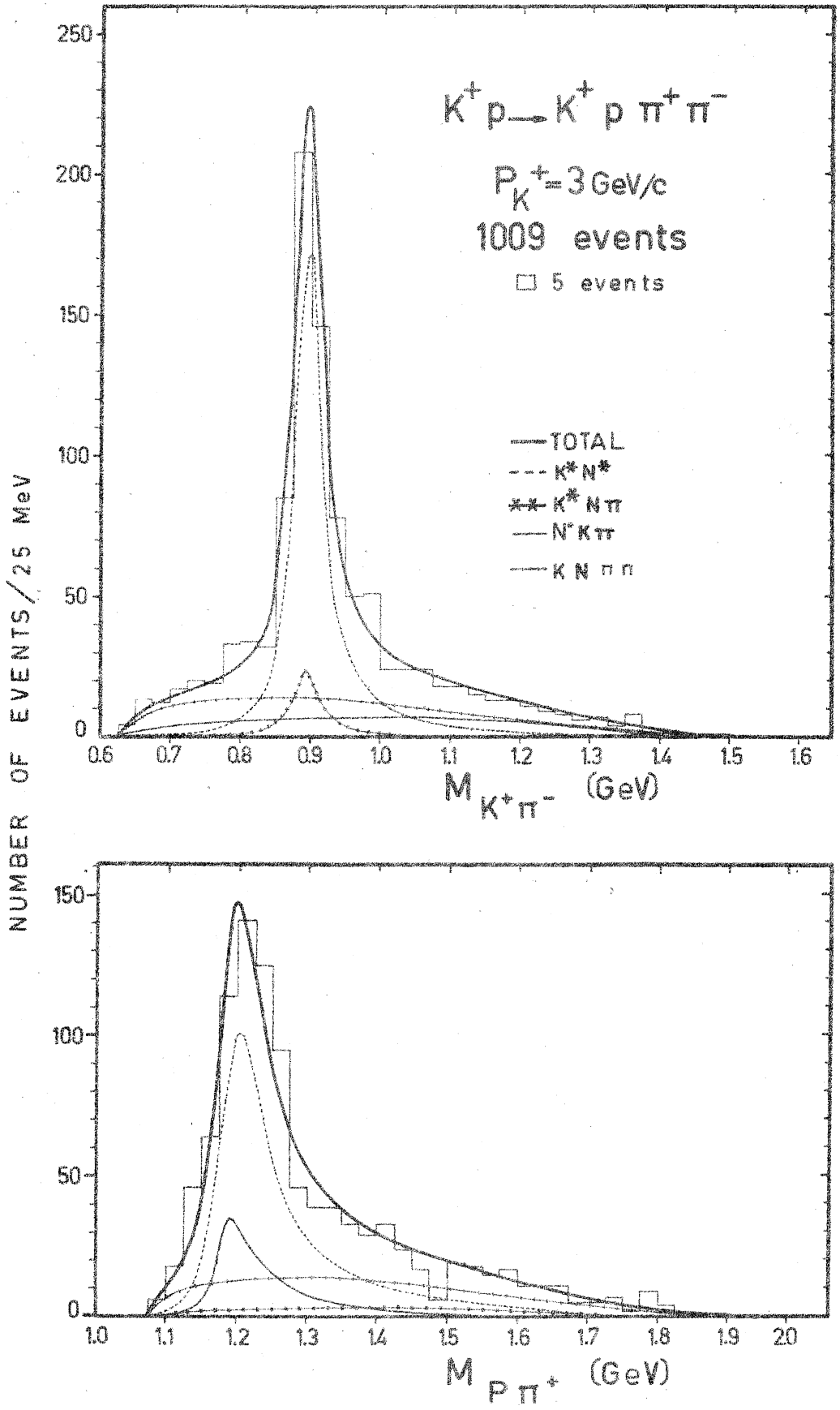

FIG. 3

DIA 22295

PS/4801/mhg

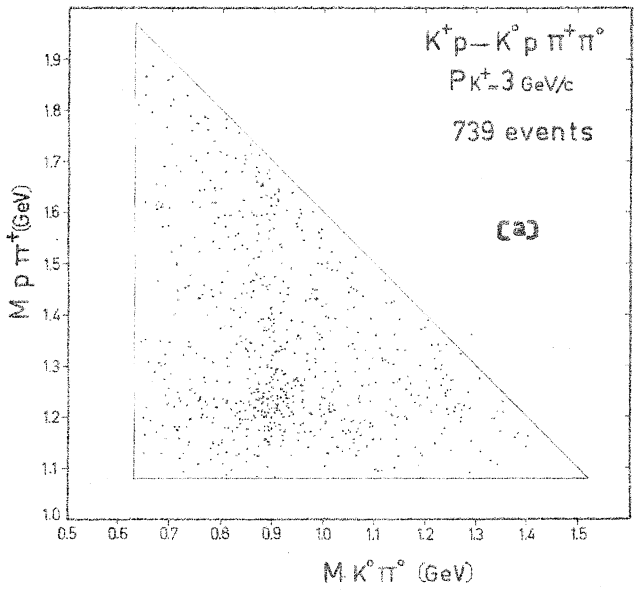
$K^+p \to K^0 p \pi^+\pi^0$
$P_{K^+} \simeq 3$ GeV/c
739 events
(a)
M p π⁺(GeV)
M K°π° (GeV)

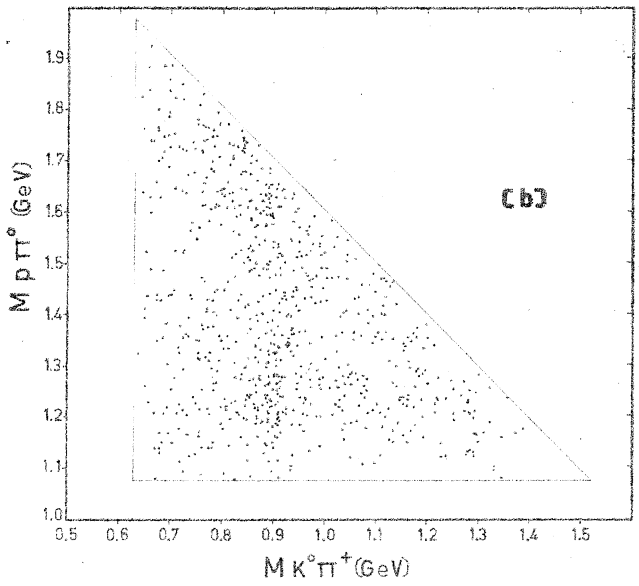
(b)
M p π° (GeV)
M K°π⁺(GeV)

PS/4807/mhg

DIR. 22293

PS/K807/nc/hg

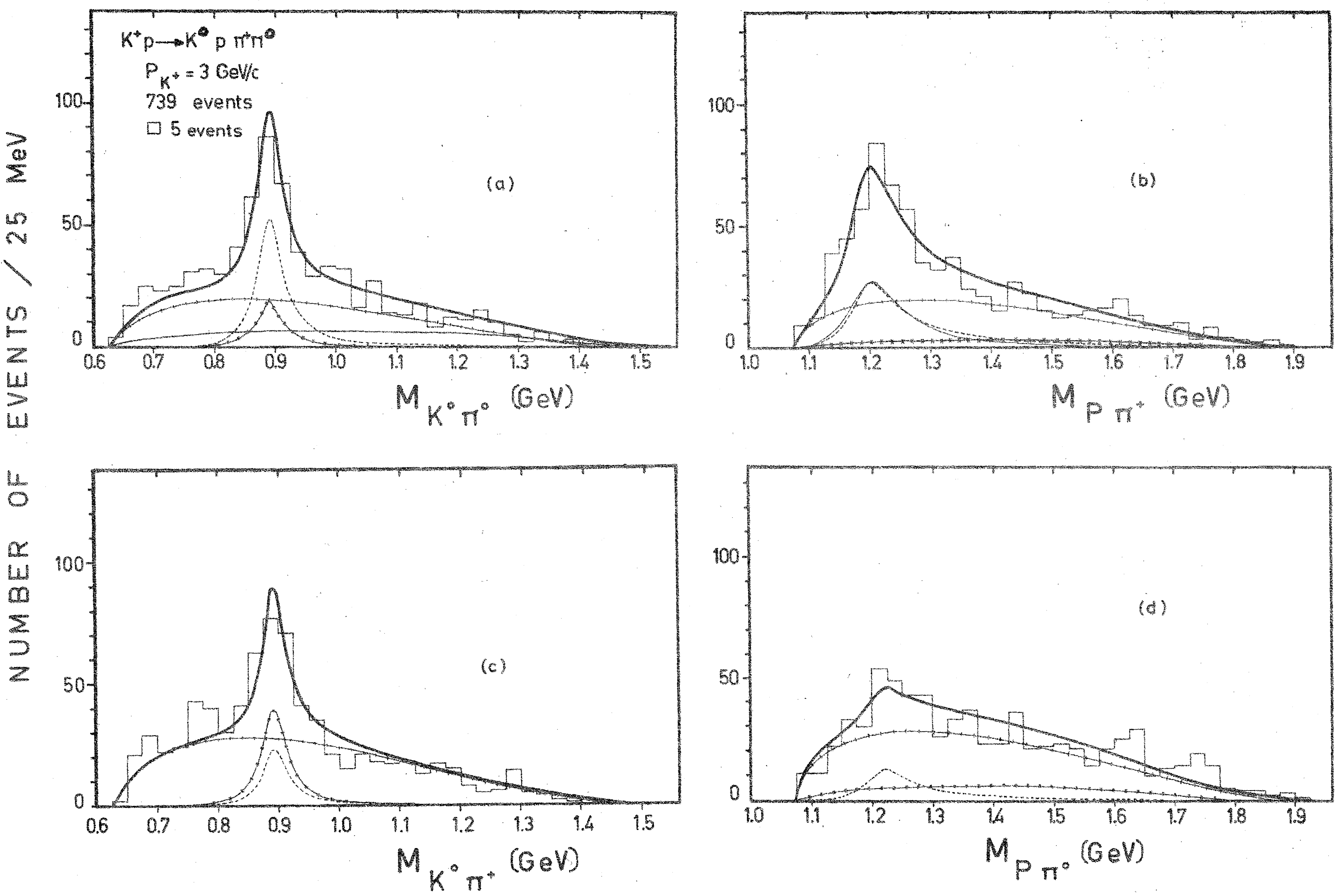

FIG. 5

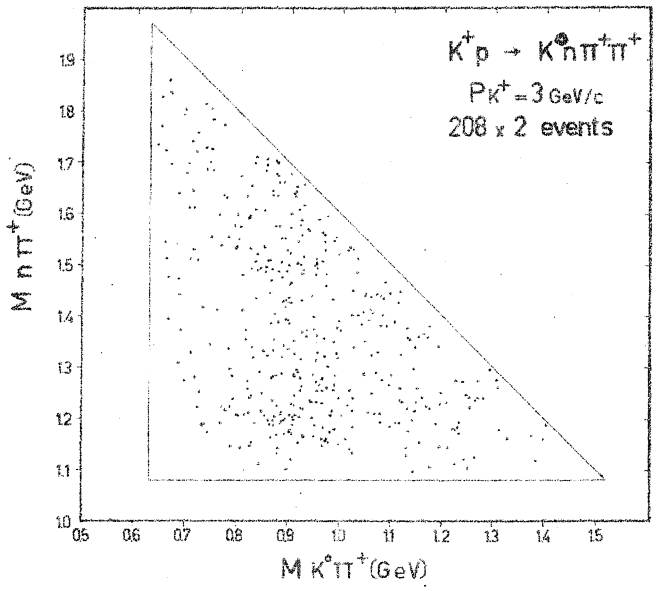

FIG. 6

PS/4801/mdg

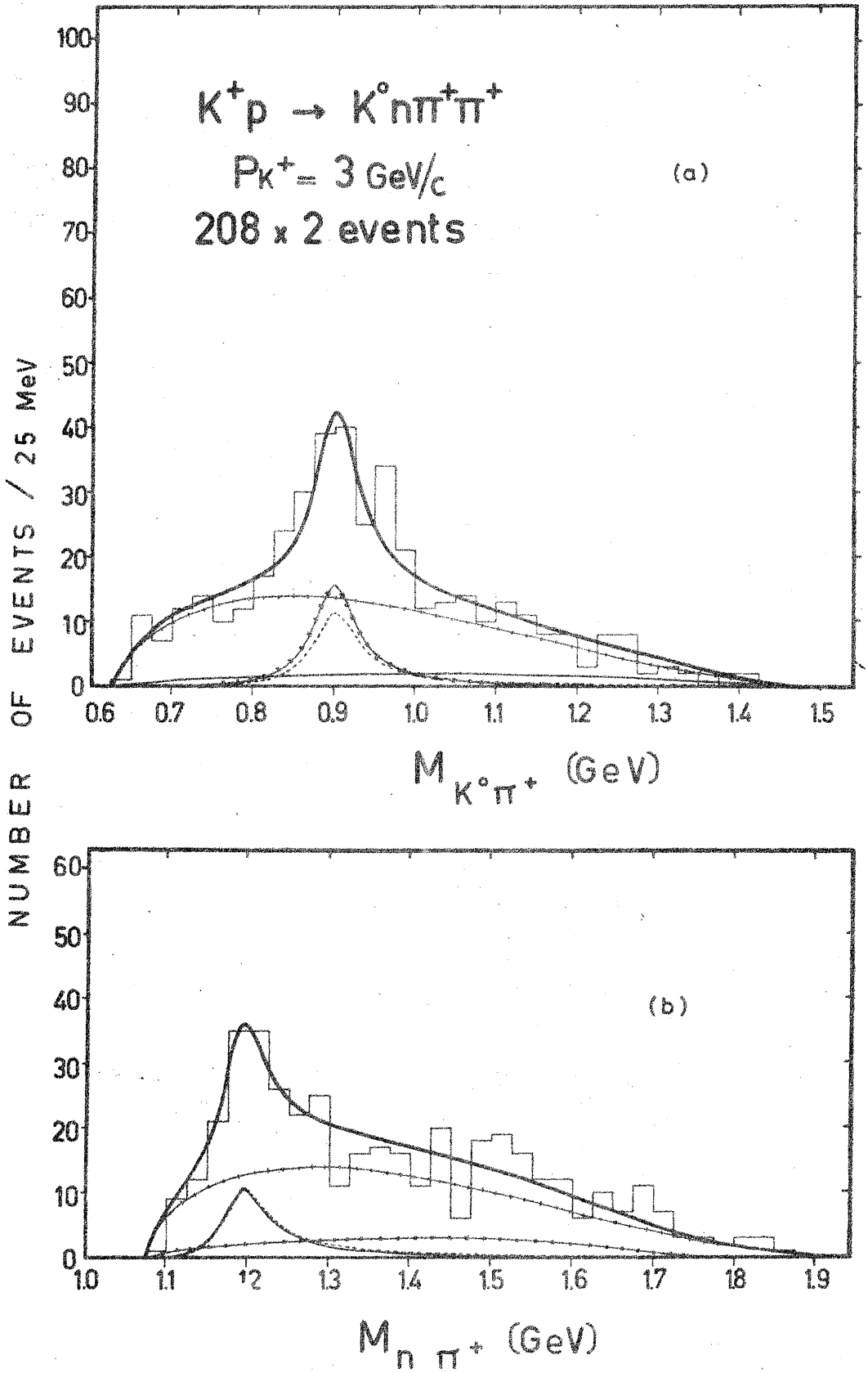

DIA. 22290
PS/4801/mhg

FIG. 7

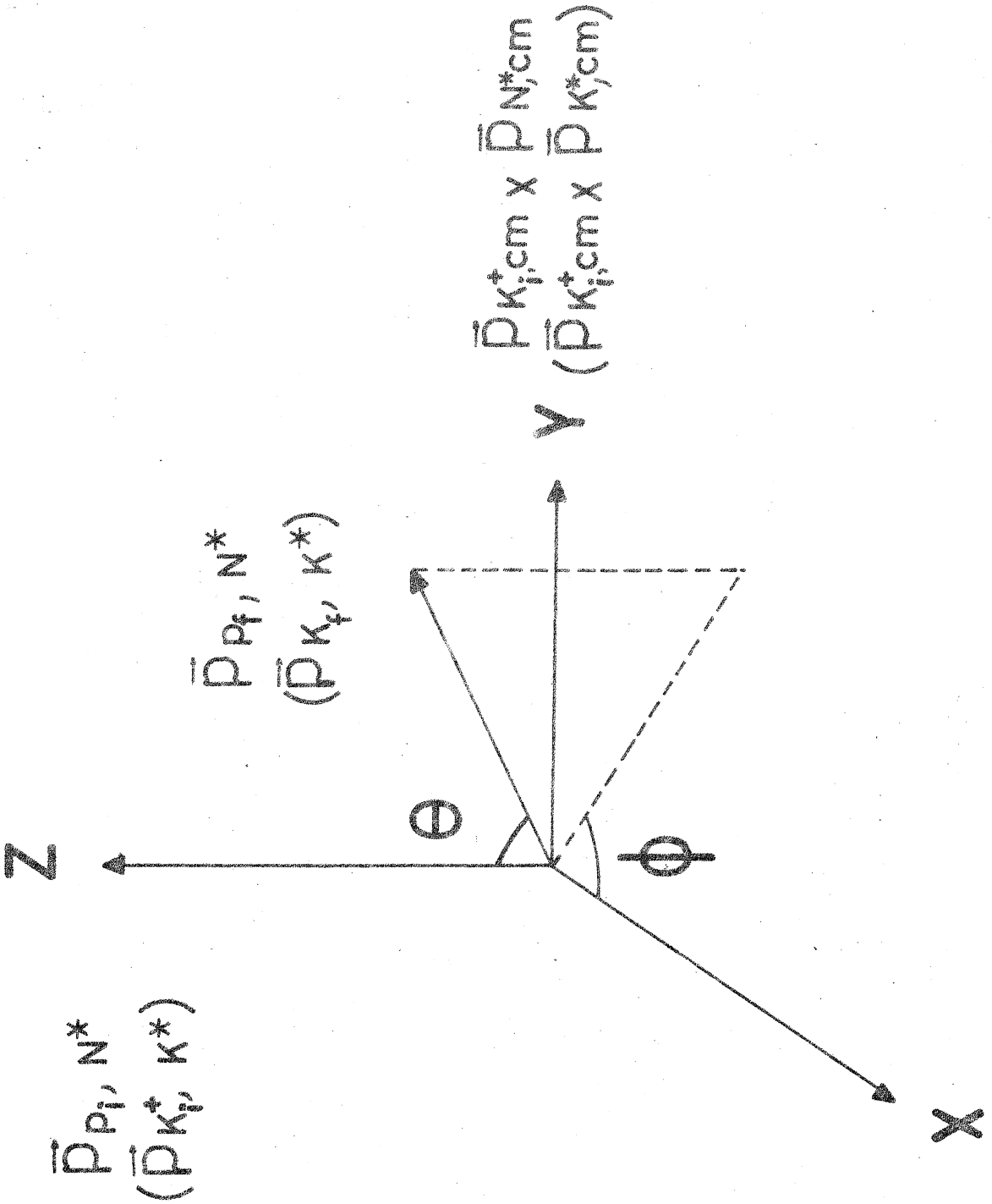

DIA 21325
PS/4807/mhg

FIG. 8

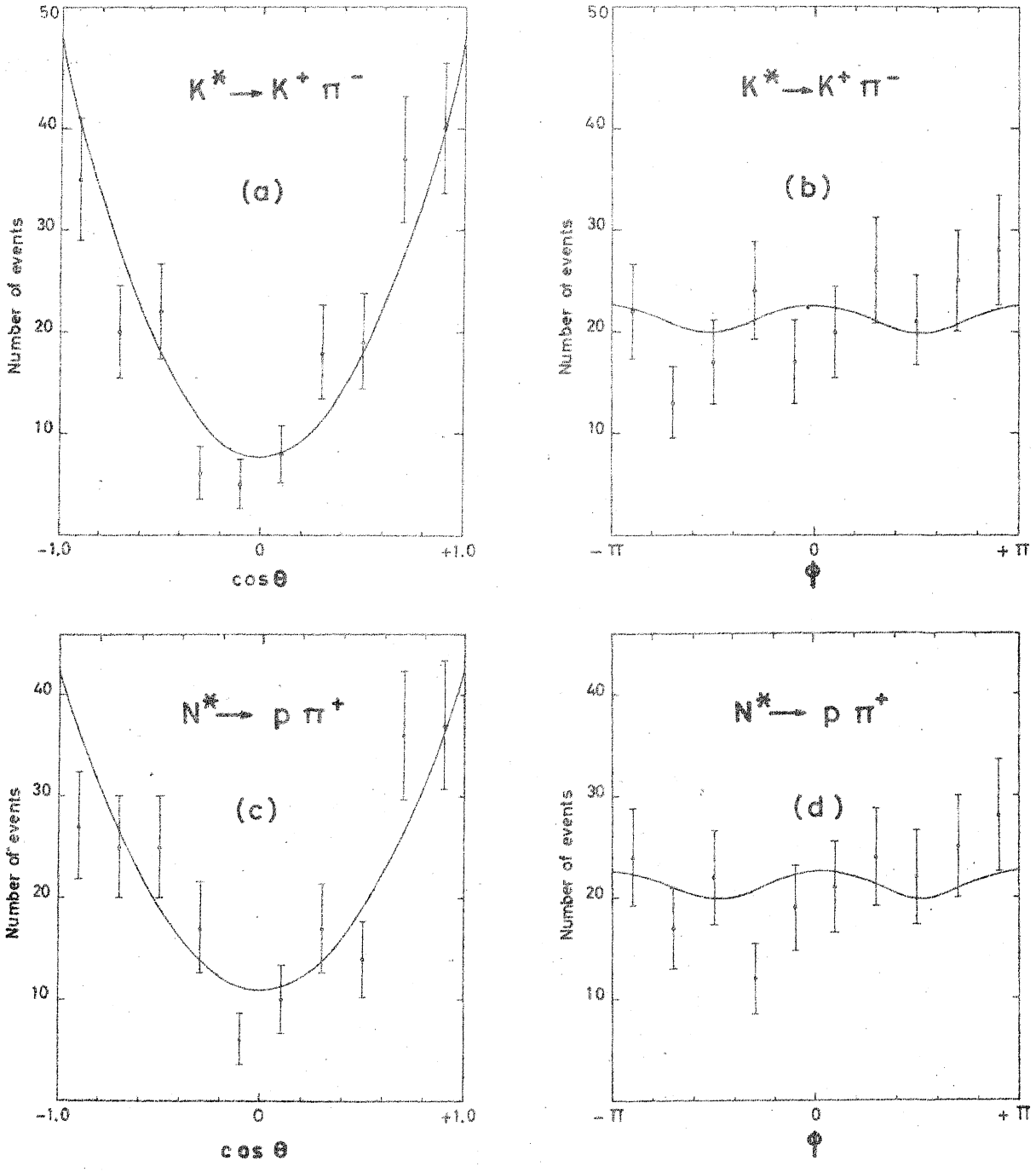

DIR. 22292
PS/4801/mhg

FIG. 9

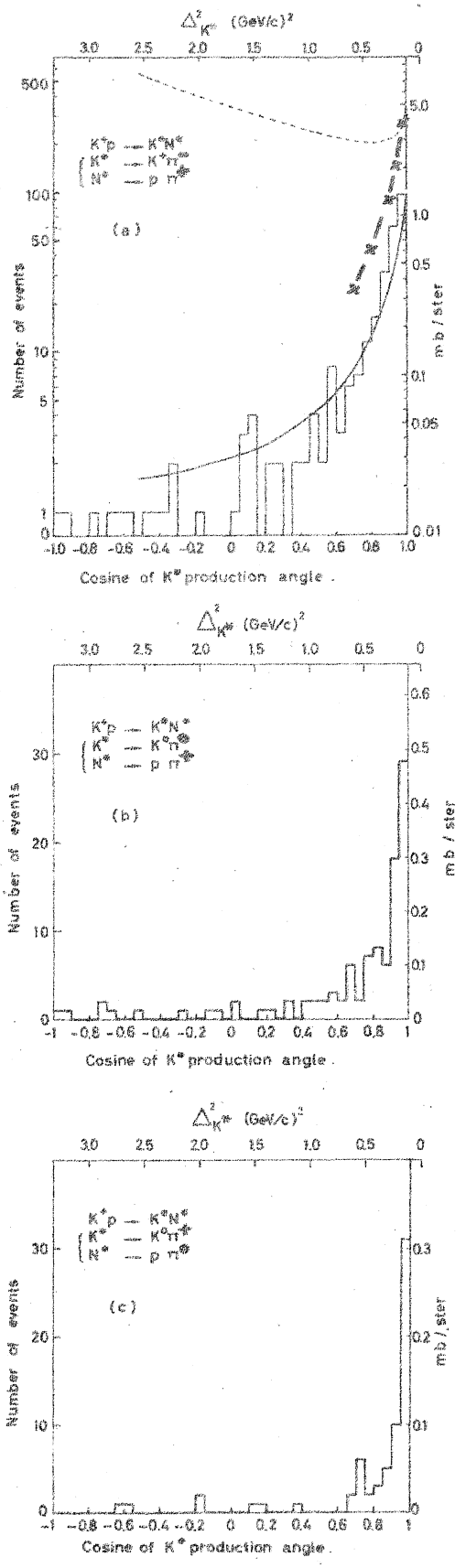

DIA. 22294
PS/4801/mhg

FIG. 10

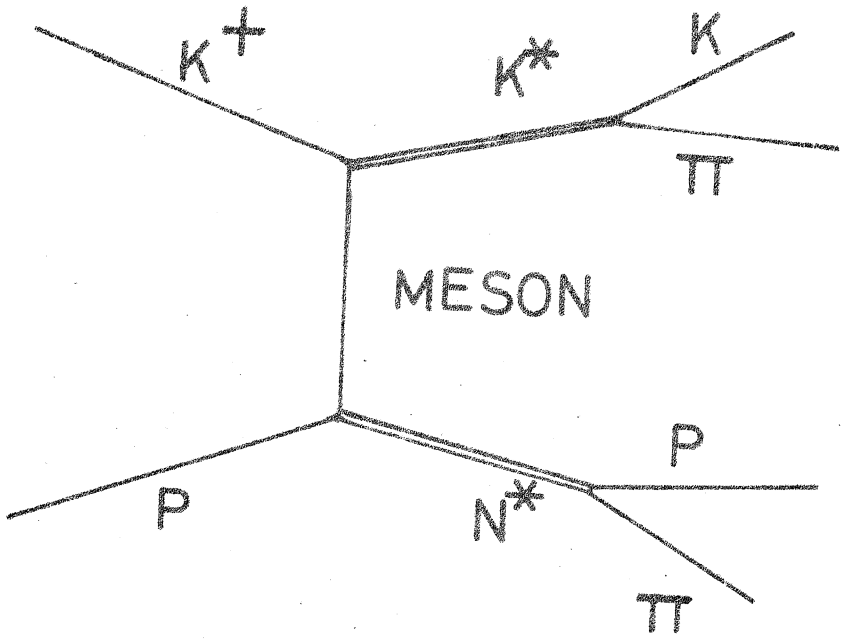

PS/4801/mhg

FIG. 11

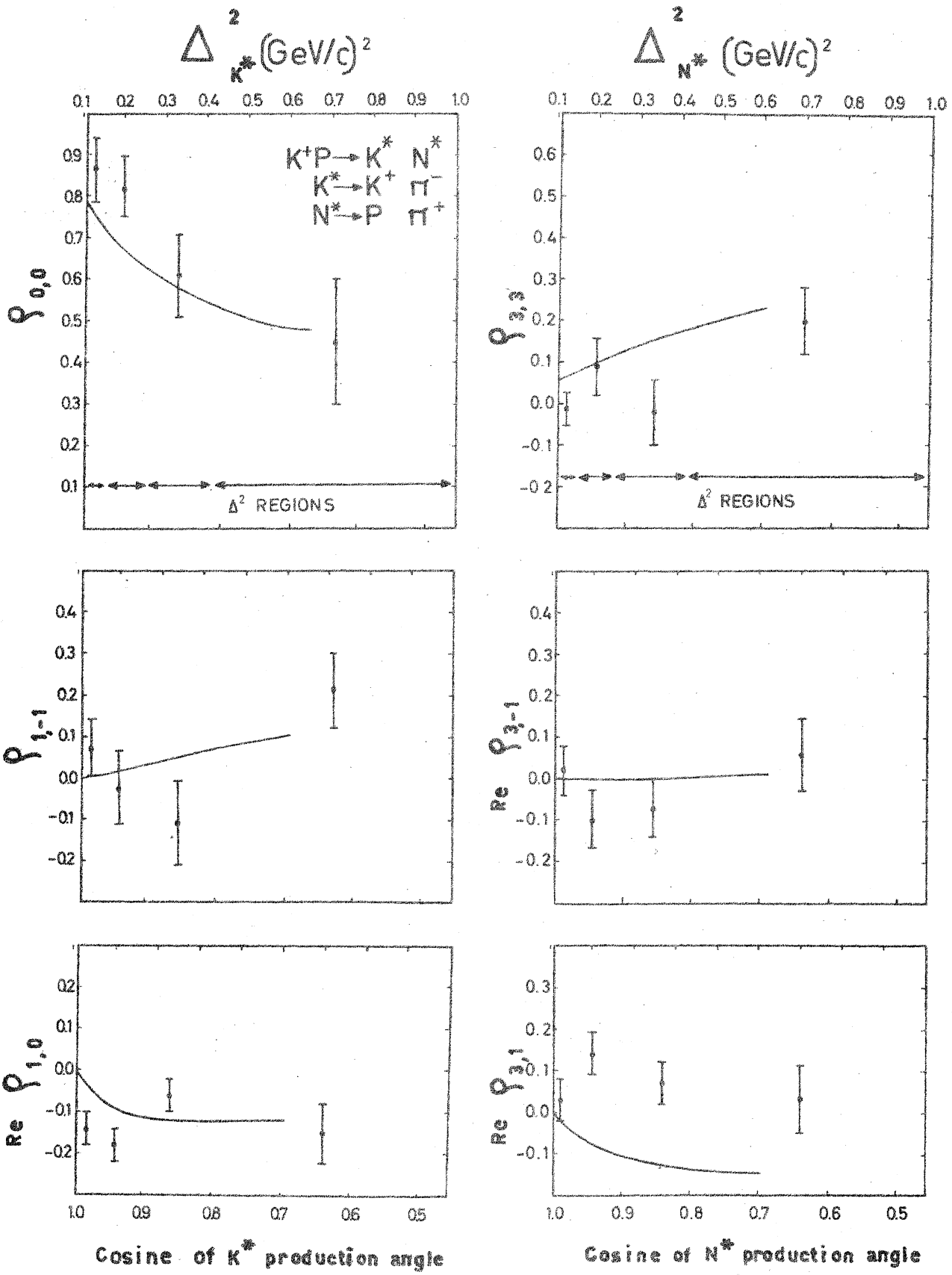

DIA 21425
PS/4807/mhg

FIG. 12